

Few-cycle oscillator pulse train with constant carrier-envelope- phase and 65 as jitter

Stefan Rausch^{1,2*}, Thomas Binhammer³, Anne Harth^{1,2}, Emilia Schulz^{1,2}, Martin Siegel^{1,2}, and Uwe Morgner^{1,2,4}

¹*Institute of Quantum Optics, Leibniz Universität Hannover, Welfengarten 1, D-30167 Hannover, Germany*

²*Centre for Quantum Engineering and Space-Time Research (QUEST), Welfengarten 1, D-30167 Hannover, Germany*

³*VENTEON Laser Technologies GmbH, D-30827 Garbsen, Germany*

⁴*Laser Zentrum Hannover e.V., Hollerithallee 8, D-30419 Hannover, Germany*

rausch@iqo.uni-hannover.de

Abstract: We report on an octave-spanning Ti:sapphire laser oscillator stabilized to carrier-envelope-offset frequency zero, generating a pulse train with constant field profile for every pulse. Stabilization is realized using an extended self-referenced locking scheme enabling to lock the carrier-envelope-offset phase with less than 65 attosecond rms timing jitter. The stabilized system features a pulse repetition rate of 100 MHz with pulses as short as 4.5 fs and 220 mW average output power. With this laser system it was possible for the first time to demonstrate a spectral interference pattern of 10^{11} oscillator pulses in an out-of-loop f -to- $2f$ -interferometer.

© 2009 Optical Society of America

OCIS codes: (120.3940) Metrology; (320.7090) Ultrafast lasers; (320.7160) Ultrafast technology.

References and links

1. G. G. Paulus, F. Grasbon, H. Walther, P. Villoresi, M. Nisoli, S. Stagira, E. Priori, and S. De Silvestri, "Absolute-phase phenomena in photoionization with few-cycle laser pulses," *Nature* **414**, 182–184 (2001).
2. O. D. Mücke, T. Tritschler, M. Wegener, U. Morgner, and F. X. Kärtner, "Determining the carrier-envelope offset frequency of 5-fs pulses with extreme nonlinear optics in ZnO," *Opt. Lett.* **27**, 2127–2129 (2002).
3. A. Baltuska, Th. Udem, M. Uiberacker, M. Hentschel, E. Goulielmakis, Ch. Gohle, R. Holzwarth, V. S. Yakovlev, A. Scrinzi, T. W. Hänsch, and F. Krausz, "Attosecond control of electronic processes by intense light fields," *Nature* **421**, 611–615 (2003).
4. A. Marian, M. C. Stowe, J. R. Lawall, D. Felinto, J. Ye, "United Time-Frequency Spectroscopy for Dynamics and Global Structure," *Science* **306**, 2063–2068 (2004).
5. A. Apolonski, P. Dombi, G. G. Paulus, M. Kakehata, R. Holzwarth, Th. Udem, Ch. Lemell, K. Torizuka, J. Burgdörfer, T.W. Hänsch, and F. Krausz, "Observation of Light-Phase-Sensitive Photoemission from a Metal," *Phys. Rev. Lett.* **92**, 073902 (2004).
6. P. A. Roos, X. Li, J. A. Pipis, T. M. Fortier, S. T. Cundiff, R. D. R. Bhat, and J. E. Sipe, "Characterization of carrier-envelope phase-sensitive photocurrent injection in a semiconductor," *J. Opt. Soc. Am.* **22**, 362–368 (2005).
7. O. D. Mücke, T. Tritschler, M. Wegener, U. Morgner, F. X. Kärtner, G. Khitrova, and H. M. Gibbs, "Carrier-wave Rabi flopping: role of the carrier-envelope phase," *Opt. Lett.* **29**, 2160–2162 (2004).
8. C. Jirauschek, L. Duan, O. D. Mücke, F. X. Kärtner, M. Wegener, and U. Morgner, "Carrier-envelope phase-sensitive inversion in two-level systems," *J. Opt. Soc. Am. B* **22**, 2065–2075 (2005).
9. T. Nakajima and S. Watanabe, "Effects of the Carrier-Envelope Phase in the Multiphoton Ionization Regime," *Phys. Rev. Lett.* **96**, 213001 (2006).

10. M. Kre, T. Löffler, M. D. Thomson, R. Dörner, H. Gimpel, K. Zrost, T. Ergler, R. Moshhammer, U. Morgner, J. Ullrich, and H. G. Roskos, "Determination of the carrier-envelope phase of few-cycle laser pulses with terahertz-emission spectroscopy," *Nat. Phys.* **2**, 327–331 (2006).
11. H. R. Telle, G. Steinmeyer, A. E. Dunlop, J. Stenger, D. H. Sutter, U. Keller, "Carrier-envelope offset phase control: A novel concept for absolute optical frequency measurement and ultrashort pulse generation," *Appl. Phys. B* **69**, 327–332 (1999).
12. D. J. Jones, S. A. Diddams, J. K. Ranka, A. Stentz, R. S. Windeler, J. L. Hall, S. T. Cundiff, "Carrier-Envelope Phase Control of Femtosecond Mode-Locked Lasers and Direct Optical Frequency Synthesis," *Science* **288**, 635–639 (2000).
13. Y. S. Lee, J. H. Sung, C. H. Nam, T. J. Yu, and K.-H. Hong, "Novel method for carrier-envelope-phase stabilization of femtosecond laser pulses," *Opt. Express* **13**, 2969–2976 (2005).
14. C. Grebing, S. Koke, and G. Steinmeyer, "Self-referencing of optical frequency combs," *CLEO 2009, CTuK5* (2009).
15. C. Grebing, S. Koke, B. Manschwetus, and G. Steinmeyer, "Performance comparison of interferometer topologies for carrier-envelope phase detection," *Appl. Phys. B* **95**, 81–84 (2009).
16. O. Mücke, R. Ell, A. Winter, J.-W. Kim, J. Birge, L. Matos, and F. X. Kärtner, "Self-Referenced 200 MHz Octave-Spanning Ti:Sapphire Laser with 50 Attosecond Carrier-Envelope Phase Phase Jitter," *Opt. Express* **13**, 5163–5169 (2005).
17. S. Rausch, T. Binhammer, A. Harth, J. W. Kim, R. Ell, F. X. Kärtner, and U. Morgner, "Controlled waveforms on the single-cycle scale from a femtosecond oscillator," *Opt. Express* **16**, 9739–9745 (2008).
18. F. X. Kärtner, U. Morgner, R. Ell, T. Schibli, J. G. Fujimoto, E. P. Ippen, V. Scheuer, G. Angelow, and T. Tschudi, "Ultrabroadband double-chirped mirror pairs for generation of octave spectra," *J. Opt. Soc. Am. B* **18**, 882–885 (2001).
19. J. Son, J. V. Rudd, and J. F. Whitaker, "Noise characterization of a self-mode-locked Ti:sapphire laser," *Opt. Lett.* **17**, 733–735 (1992).
20. F. W. Helbing, G. Steinmeyer, and U. Keller, "Carrier-envelope offset phase-locking with attosecond timing jitter," *IEEE J. Sel. Top. Quantum Electron.* **9**, 1030–1040 (2003).
21. H. M. Crespo, J. R. Birge, E. L. Falcão-Filho, M. Y. Sander, A. Benedick, and F. X. Kärtner, "Nonintrusive phase stabilization of sub-two-cycle pulses from a prismless octave-spanning Ti:sapphire laser," *Opt. Lett.* **33**, 833–835 (2008).
22. C. Manzoni, C. Vozzi, E. Benedetti, G. Sansone, S. Stagira, O. Svelto, S. De Silvestri, M. Nisoli, and G. Cerullo, "Generation of high-energy self-phase-stabilized pulses by difference frequency generation followed by optical parametric amplification," *Opt. Lett.* **31**, 963–965 (2006).
23. S. Adachi, N. Ishii, T. Kanai, A. Kosuge, J. Itatani, Y. Kobayashi, D. Yoshitomi, K. Torizuka, and S. Watanabe, "5-fs, multi-mJ, CEP-locked parametric chirped-pulse amplifier pumped by a 450-nm source at 1 kHz," *Opt. Express* **16**, 14341–14352 (2008).

1. Introduction

Within the last decade developments and achievements in terms of few-cycle laser pulse generation have led to numerous fields of research and applications such as high precision metrology, high-harmonic generation, attosecond science, and high-field physics. For pulse durations approaching the single-cycle limit thereby the influence of the electric field determined by its carrier-envelope-offset phase (CEP) became apparent [1–10].

Meanwhile CEP stabilization is done routinely by using self-referencing f -to- $2f$ -interferometers [11, 12]. Applying this locking scheme, pulses of a mode-locked laser are usually stabilized to an n^{th} -fraction of the lasers' repetition rate, giving an identical electric field for every n^{th} pulse within the generated pulse train.

For some applications sensitive to the field profile of the applied pulses, a pulse train with identical electric field properties is essential. This is implemented in amplified laser systems simply by picking an integer multiple of n from the pulse train at kHz-rates and applying a second slow feedback loop [3].

Locking of the oscillator directly to $f_{CE} = 0$ cannot be realized using the standard self-referencing locking scheme which is based on measuring f_{CE} separated from the pulse repetition frequency. To overcome this problem Lee et al. proposed a 'direct locking method' in the time domain [13] and recently a novel method to lock f_{CE} to zero without affecting the oscillator was introduced by Grebing et al. [14]. Here the first order of an acousto-optic frequency

shifter (AOFS) within the output beam is used to shift the instantaneous CE frequency directly to zero. The necessary f_{CE} beat signal which is applied to the AOFS is measured using a common path f -to- $2f$ -interferometer [15]. This locking technique is advantageous compared to the commonly used phase coherent locking technique in terms of leaving the oscillator untouched - no direct feedback like pump-power modulation or mirror translation is required. The main drawback of this method is using the first diffraction order of the AOFS as applicable output affecting the beam in terms of temporal and angular dispersion.

Here, we report on an octave-spanning Ti:sapphire oscillator stabilized to carrier-envelope-offset frequency zero using a modified f -to- $2f$ self-referencing locking scheme in the frequency domain, generating a pulse train with constant CEP at a pulse duration as short as 4.5 fs. The measured in-loop residual rms phase noise is 164 mrad (integrated from 3 MHz to 3 Hz) resulting in a CE timing jitter of 65 as. Due to the octave-spanning output spectrum only 10 % of the original average output power has to be abandoned for the CEP lock and 220 mW remain in unchanged beam quality for subsequent experiments.

With this system it was possible for the first time to record an interference of 10^{11} oscillator pulses in an out-of-loop interferometer, proving an excellent CEP lock.

2. Laser system

The laser system is a prism-less Ti:sapphire laser (VENTEON — PULSE : ONE OS) designed for soft aperture Kerr-lens mode-locking (see e.g. [16, 17]). Pumping is done by 532 nm cw-radiation from a frequency doubled Nd:YVO₄ laser (Coherent Verdi series). For intracavity dispersion management, broadband double chirped mirror pairs (DCMPs, [18]) are used together with BaF₂-substrates, leading to the octave-spanning spectrum, shown in Fig. 1(A).

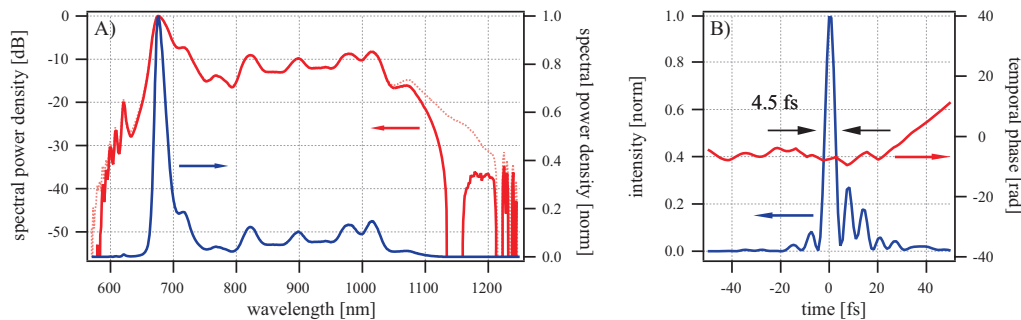


Fig. 1. Oscillator output characteristics: A) Octave-spanning output spectrum shown on a logarithmic (left, red) and linear scale (right, blue). The dotted logarithmic spectrum illustrates the full oscillator spectrum, whereas the solid one gives the spectrum remaining for experiments after CEP stabilization. B) SPIDER-characterized CEP-stabilized pulse with a duration of 4.5 fs (FWHM).

This spectrum supports a Fourier-limited pulse duration as short as 4.1 fs for the full available spectral width (Fig. 1(A): dotted red line) and 4.3 fs for the spectrally filtered case, where the spectral wings needed for CEP stabilization are already extracted (solid red line). After this filtering, still the laser features an average output power of about 220 mW at a pulse repetition rate of 100 MHz resulting in a CEP-stabilized pulse energy of approx. 2.2 nJ. After extra cavity compression with DCMPs, the phase-stabilized pulses were characterized with a home-built SPIDER system to be as short as 4.5 fs, given in Fig. 1(B).

3. Carrier-envelope-offset frequency to zero stabilization

The spectral width of the laser system is sufficient to realize CEP stabilization without any additional spectral broadening using the f -to- $2f$ self-referencing technique [11, 12].

For generating the f -to- $2f$ beat signal the spectral wings centered around 570 nm and 1140 nm are filtered from the output spectrum using a multichroic transmission filter, see Fig. 2 (left). Due to the characteristics of this filter only approx. 10% of the original laser output power is coupled into the f -to- $2f$ -interferometer. The center part of the spectrum is reflected with unchanged beam quality and remains for subsequent experiments. Within the interferometer the f and $2f$ frequency components are separated using a dichroic beam splitter (DBS). In this interferometer configuration the $2f$ components around 570 nm are reflected whereas the f components around 1140 nm are transmitted. For optimizing the heterodyne beat signal, one arm can be tuned in terms of polarization and delay with respect to the second one to allow for interference on a highly sensitive avalanche photodiode (Menlo Systems APD210) after doubling in a nonlinear type-I-crystal (1 mm LBO).

As mentioned earlier this locking scheme is not appropriate to lock f_{CE} to zero because there is no way to measure this frequency without excessive DC-noise contributions. Based on a suggestion by Jones et al. [12] here an additional acousto-optic frequency shifter (AOFS) was integrated in one interferometer arm shifting the measured CE-frequency f_{CEm} at the photodiode according to

$$f_{CEm} = f_{CE} \pm f_{AOFS}. \quad (1)$$

In our case the signal is shifted relative to the laser repetition rate f_{rep} by $f_{AOFS} = 80$ MHz resulting in a beat signal of $f_{CEm} = 20$ MHz for $f_{CE} \approx 0$. For all these considerations f_{rep} serves as a reference point.

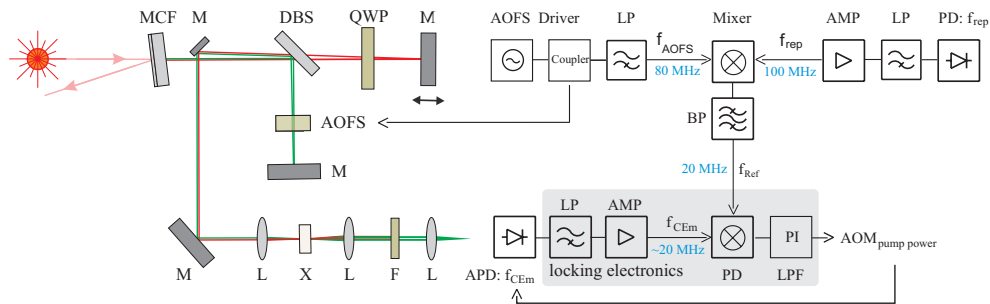


Fig. 2. Locking f_{CE} to zero; Left: Extended f -to- $2f$ interferometer setup - AOFS: acousto-optic frequency shifter; APD: avalanche photo diode; DBS: dichroic beam splitter, F: interference filter, L: focusing lens, M: mirror, MCF: multichroic filter, QWP: quarter wave plate, X: SHG crystal; Right: RF-locking-scheme - the locking reference f_{Ref} is generated by mixing the AOFS driving frequency $f_{AOFS} = 80$ MHz with the lasers' repetition rate $f_{rep} = 100$ MHz down to 20 MHz. f_{CE} -locking is accomplished by a PLL controlling the lasers' pump power; AMP: amplifier, BP: bandpass filter, LP: lowpass filter, LPF: loop filter, PD: phase detector.

The setup of the advanced f -to- $2f$ -interferometer - extended by the AOFS - is given in Fig. 2 (left). The AOFS is made of dense flint glass, introducing only a reasonable amount of dispersion into the setup and provides a constant shift of 80 MHz to the frequencies contained in this arm. The $2f$ components pass the AOFS in a collimated beam with a radius of approx. 1 mm. The efficiency diffracted into the 1st order, carrying the frequency shifted signal, is in

the order of 50 % but still sufficient to achieve a beat signal with a signal-to-noise ratio (SNR) greater than 30 dB in a 100 kHz resolution bandwidth. This signal allows for stabilization of the oscillator using the phase-locked loop (PLL, Menlo Systems XPS) controlling the pump power via an acousto-optic modulator. The rather low diffraction efficiency of the AOFS can only be tolerated within the fundamental arm of the interferometer, at which reasonable initial signal intensity is available at 570 nm.

For generating a pulse train with constant CEP the locking reference f_{Ref} is an essential parameter which has to account for fluctuations of the laser repetition rate and the AOFS driving frequency as well. In our case f_{Ref} is generated by mixing f_{AOFS} at 80 MHz with f_{rep} at 100 MHz down to a signal located at 20 MHz. This scheme is shown schematically in Fig. 2 (right). After bandpass filtering, f_{Ref} serves as reference for locking the measured (shifted) f_{CEm} signal using a phase-locked loop. By including f_{AOFS} and f_{rep} in this reference, their fluctuations - also affecting f_{CE} - will cancel out.

An in-loop measurement based on this scheme is shown in Fig. 3 (A). It is recorded in a 100 Hz span with a device-limited resolution bandwidth of 1 Hz (Agilent E4440A), exhibiting a SNR of approx. 60 dB. Figure 3 (B) gives the single sideband noise power spectral density (PSD) S_ϕ of the CEP phase fluctuations (red), next to the measurement noise floor (blue) and locking reference (green).

According to the method presented in [19] the accumulated root-mean-square (rms) CE phase error $\Delta\phi$ can be obtained from the measured S_ϕ by integrating over the frequency leading to the CE timing jitter σ_τ using

$$\sigma_\tau = \frac{1}{2\pi \cdot f_0} \cdot \Delta\phi = \frac{1}{2\pi \cdot f_0} \cdot \left[2 \int_{3\text{Hz}}^{3\text{MHz}} S_\phi(f') df' \right]^{1/2} \quad (2)$$

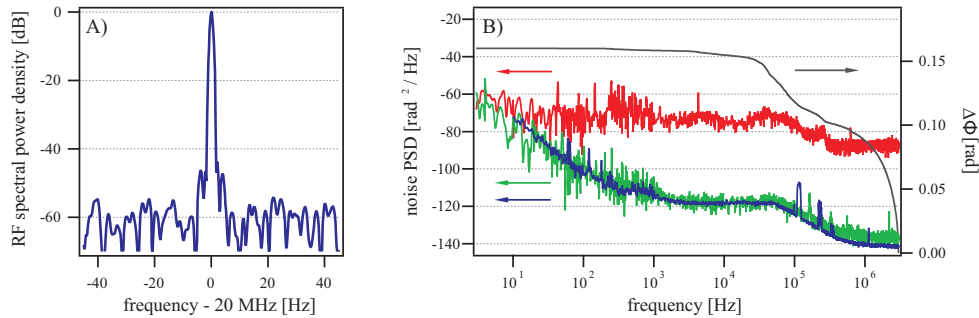


Fig. 3. In-loop characteristics; A) Stabilized f_{CEm} beat note at 20 MHz shown in a 100 Hz span with 1 Hz resolution bandwidth featuring a SNR greater than 60 dB; B) Noise PSD of CEP fluctuations (red), the locking reference (green), and measurement noise floor (blue) next to the integrated rms phase error for the CEP fluctuations (grey, right).

For our case a value of $\Delta\phi=164$ mrad results for the CEP error integrated from 3 MHz to 3 Hz giving an rms CE timing jitter of 64.5 as by relating this value to the carrier frequency f_0 at 375 THz, see Eq. 2. Similar values have been achieved for standard locking schemes with $f_{CE} = f_{rep}/4$, ranging between 10 as and 50 as [16, 20, 21].

Unfortunately, a comparison between other techniques used to stabilize f_{CE} to zero lacks from comparable characterization schemes. Lee et al. measured an in-loop rms phase error of 50 mrad (100 mrad out-of-loop) but only integrated from 0.3 Hz up to 1.5 kHz [13]. Grebing et al. intrinsically can only measure an out-of-loop signal. For their RF-analysis they obtained an residual rms phase noise of 300 mrad [14]. With the technique presented in this paper intrinsically no

out-of-loop RF-analysis can be performed because the beat signal cannot be exclusively analyzed apart from the f_{rep} beat note.

4. Out-of-loop characterization and verification of zero carrier-envelope-offset frequency

To verify and characterize the identity of subsequent field profiles, the laser output is split by an octave-spanning 50:50 beamsplitter (VENTEON) and guided into a second f -to- $2f$ -interferometer, the experimental arrangement given in Fig. 4 (left). For the out-of-loop interferometer a SNR value well above 20 dB (100 kHz RBW) is achieved. The out-of-loop signal is fiber-coupled and can be either fed to an APD detector for RF-analysis or into a highly sensitive CCD-spectrometer (ANDOR SR300i & Newton^{EM} 970) for spectral characterization. Please note that the second interferometer does not carry an AOFS and reveals the actual oscillator CE frequency and phase change.

After locking the laser, the out-of-loop f_{CE} needle vanishes within zero frequency, the f_{rep} beat note on the other hand, and is not detectable anymore, even with the highest possible resolution.

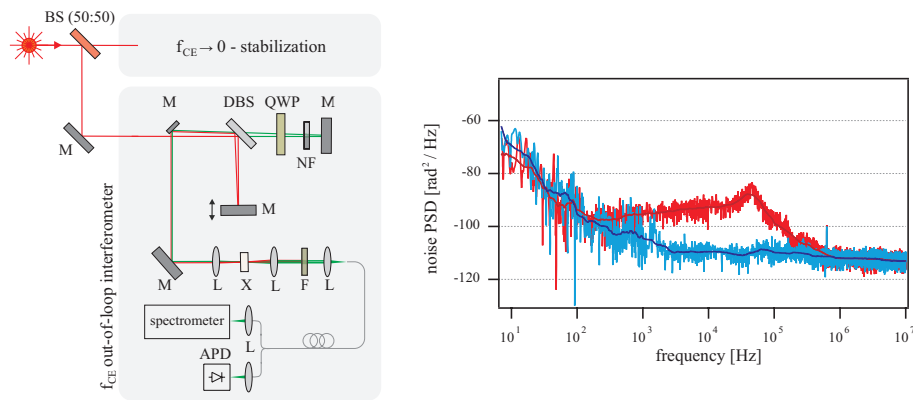


Fig. 4. Out-of-loop characterization; Left: Experimental setup - the laser output is split and launched into the main f -to- $2f$ interferometer from Fig. 2 for zero locking, and a second f -to- $2f$ -interferometer for out-of-loop characterization; BS: beam splitter, NF: neutral density filter; Right: Noise PSD of the out-of-loop f_{rep} fluctuations with locked-to-zero CE frequency for different locking settings (gain 4: red, gain 7: blue).

The noise power spectral density of the out-of-loop f_{rep} -fluctuations - including the f_{CE} -fluctuations as well - is given for two different locking settings in Fig. 4 (right). The red curve shows the noise PSD for a loose f_{CE} -lock with a loop gain of 4 whereas the blue curve gives the noise PSD for a tight lock with a gain setting of 7. In our case this is the optimal choice for locking f_{CE} . Here, the phase noise is not distinguishable from the f_{rep} -noise PSD without any f_{CE} -influence.

The final verification of a locked field profile is the visualization of the interference between the f - $2f$ frequency components in the optical spectrum as it is usually done for low repetition rate amplified pulses [22, 23]. For a typical spectrometer integration time of some milliseconds and a pulse repetition rate of 100 MHz, millions of pulses have to interfere with visible interference contrast.

Figure 5 gives to the best of our knowledge for the first time an interference progression of the f and $2f$ components of oscillator pulses. For each single underlying interferogram 10^7 oscillator pulses interfere, for the recorded time of 2500 s all together more than 10^{11} .

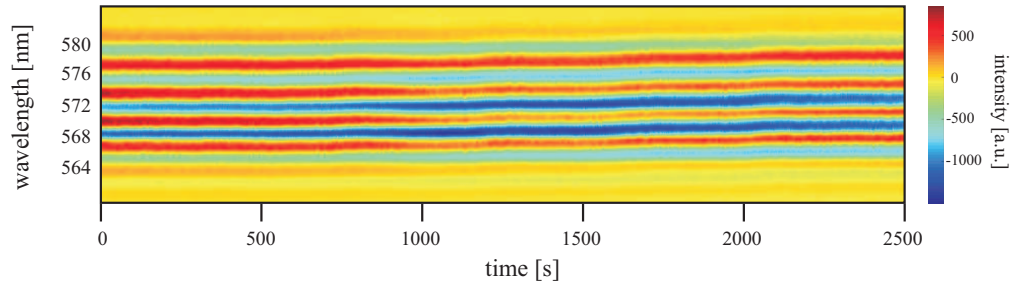


Fig. 5. Out-of-loop interference of the f and $2f$ components of the stabilized pulse train. The interference is recorded over 2500 seconds with a spectrometer integration time of 0.5 seconds.

For capturing this interference pattern, the output of the second interferometer from Fig. 4 is coupled into the CCD-spectrometer. For contrast reasons the spectral power in both interferometer arms is balanced using neutral density filters attenuating the fundamental arm. To observe a noticeable interference the delay between the two signals has to be detuned from zero about $50\ \mu\text{m}$ resulting in the interference pattern that is traced for a time sequence of 2500 s in Fig. 5. Hereby the interference contrast is highly sensitive on the locking strength and immediately vanishes with switched-off lock. The presented spectral data is corrected with respect to a background given by the single spectral components without interference.

As it can be seen in Fig. 5 there is a very slow wavelength drift of the interference pattern over time, whereas the interference contrast in general is not affected. This residual phase drift can be analyzed by Fourier-transforming the interference signal, thereby extracting the phase and tracking this value over the observation time. For the presented measurement this results in a slow phase drift of 1.7 rad accumulated over 2500 s. For a shorter time scale an accumulated phase fluctuation of approx. 360 mrad was obtained for an observation time of 200 s. These fluctuations mainly have their origin in thermal variations of the laboratory conditions since the breadboard for the laser and interferometers is not actively temperature stabilized. These even small temperature drifts can affect the relative phase between the f and $2f$ components due to dispersion resulting e.g. from minimal beam misalignment within the out-of-loop interferometer. Without any slow feedback loop as used in amplified field stable systems this behavior is not surprising at all.

Figure 6 shows a comparable interference pattern while shifting the absolute phase by moving a BaF_2 wedge through the beam. For BaF_2 a measured thickness-change of approx. $81\ \mu\text{m}$ was necessary to shift the phase by 2π , shown in the middle part of Fig. 6, which is in good agreement with the calculated value of $75\ \mu\text{m}$. The corresponding electric field profiles of the underlying ultrashort pulses given in Fig. 1 (B) are shown in the lower section of Fig. 6 for three different CEP-settings and the relevant center part of the pulse: at the time t_1 for $\text{CEP} = 0$, at t_2 for $\text{CEP} = \pi/2$ and at t_3 for $\text{CEP} = \pi$. At the time t_4 the CEP lock is switched off, the interference pattern vanishes immediately.

Please note that the above presented results give only a rough estimate of the system performance because the SNR of the in-loop measured beat note is reduced about 5 dB due to splitting the laser output power for both, stabilization and out-of-loop characterization. Thus for usual operation at full available power the performance can be assumed to be even better.

This overall system is mounted together with the pump laser on a compact and moveable board with a footprint of 900 mm times 750 mm. Currently it is in use as the driving laser to investigate quantum interference in alkaline atoms, where theory has shown that the population probability of bound atomic states depends on the CEP of the driving laser pulses. This laser

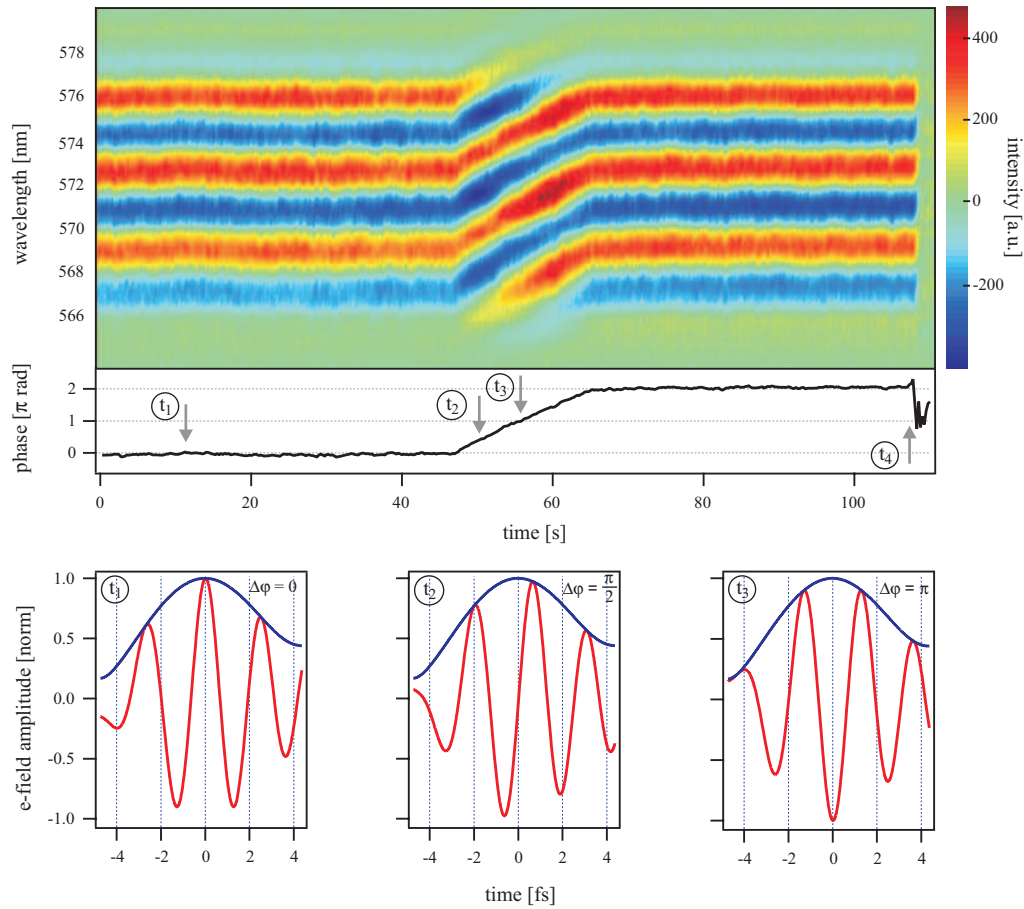


Fig. 6. CEP interference pattern while shifting the absolute phase with a BaF₂ glass wedge; Top: Out-of-loop spectral interference pattern - starting at approx. 47 s the absolute phase is shifted by steadily inserting BaF₂ into the beam. At 65 s the phase has slipped by about 2π ; Middle: Extracted phase; Bottom: Electric field profile of the center parts of the underlying pulses at three different times t_1 , t_2 and t_3 with assumed CEP=0 as starting point. At t_4 the lock is switched off.

source represents a light source with sub-two-cycle pulses with constant CEP that allows for integration times of several seconds together with an octave-spanning spectrum with reasonable power for the atomic excitation. Next to this, the CEP dependency of two-photon photoemission (2PPE) from metals will be subject of investigations.

5. Conclusion

In conclusion, we demonstrated for the first time an octave-spanning Ti:sapphire laser oscillator stabilized with respect to carrier-envelope-offset frequency zero, delivering a pulse train with stable and identical field profiles. The measured rms timing jitter of the CE phase fluctuations is smaller than 65 attoseconds allowing for the first time to investigate the interference of oscillator pulses at 100 MHz repetition rate. The excellent beam quality and 220 mW usable average output power make this laser the ideal source for field sensitive experiments at high repetition rates as well as for broadband CEP stable amplifier seeding.

Acknowledgements

The authors thank VENTEON Femtosecond Laser Technologies GmbH for supporting the development and assembling of the laser oscillator, Oliver D. Mcke and Oliver Prochnow for some fruitful discussions and Jens Gdde, Marcel Krenz, and Martin Wolf for motivating this system.

The work was financially supported by the DFG collaborative research center (SFB) 407 and the DFG cluster of excellence "Centre for Quantum Engineering and Space-Time Research" (QUEST).